A Numerical Analysis of the Spectrum of the Almost Mathieu Operator

by

SUNMI YANG

Mihai Stoiciu, Advisor

A Thesis
Submitted in partial fulfillment
of the requirements for the Degree of Bachelor of Arts with Honors
in Mathematics

WILLIAMS COLLEGE

Williamstown, Massachusetts

19 May 2008

I would like to thank Dr. Mihai Stoiciu for his tireless patience and guidance through this whole process, and Haydee Lindo and Amy Steele for their encouragement and sense of humor during the countless late nights in Jesup. Many thanks also to Jodi Gajadar for letting me crash on her floor in West and for waking me up when I failed to hear the alarm, and Christina Rabadan for providing tissues when I caught Jodi's plague (from sleeping on her floor). Finally, I would like to thank my family, without whose love and support none of this would have been possible.

Contents

List of Figures

Chapter 1

Introduction

1.1 The Ten Martini Problem

The Schrödinger operator on $l^2(\mathbb{Z})$

$$(H_{\lambda,\alpha,\theta}u)_n = u_{n+1} + u_{n-1} + 2\lambda\cos 2\pi(\theta + n\alpha)u_n \tag{1.1}$$

with $\lambda, \theta, \alpha \in \mathbb{R}$ where $\lambda \neq 0$ and α is irrational, is called *almost Mathieu*. In his AMS talk in 1981, Mark Kac offered ten martinis to anyone who could prove that the spectrum $\sigma(H_{\lambda,\alpha})$ of the almost Mathieu operator is a Cantor set.

Definition 1.1 (Cantor set [1])**.** *Let C be a Cantor set. Then C is a closed, uncountable set consisting entirely of boundary points. That is,*

1. *C is compact, nowhere dense, and totally disconnected (i.e., the only connected subsets of C are single points). Moreover, C has no isolated points.*
2. *The measure of C is 0.*
3. *The cardinality of C is $\mathfrak{c}$.*

The most famous example of a Cantor set is the ternary set T_∞, also called the Cantor comb or the "no middle third" set [2].

Example 1.2. *To construct the Cantor set T_∞, start with the interval $[0,1] = T_0$. Remove the open middle third $(\frac{1}{3}, \frac{2}{3})$ of T_0, then the middle thirds $(\frac{1}{9}, \frac{2}{9})$ and $(\frac{7}{9}, \frac{8}{9})$ of the two pieces of T_1, and continue this procedure ad infinitum to obtain*

$$\begin{aligned}
T_0 &= [0,1] \\
T_1 &= \left[0, \frac{1}{3}\right] \cup \left[\frac{2}{3}, 1\right] \\
T_2 &= \left[0, \frac{1}{9}\right] \cup \left[\frac{2}{9}, \frac{1}{3}\right] \cup \left[\frac{2}{3}, \frac{7}{9}\right] \cup \left[\frac{8}{9}, 1\right] \\
&\vdots \\
T_n &= \frac{T_{n-1}}{3} \cup \left(\frac{2}{3} + \frac{T_{n-1}}{3}\right)
\end{aligned}$$

Thus we have the set of points in [0,1] whose ternary expansions do not contain 1.

A partial solution to the Ten Martini Problem was published in 2003 by Puig, who showed that the spectrum of the almost Mathieu operator for Diophantine α is a Cantor subset of the real line [3]. However, a more complete solution, encompassing all irrational α, was forthcoming.

Jitomirskaya showed in 1999 [4] that the spectrum of the almost Mathieu operator is

1. purely absolutely continuous for $\lambda < 2$;
2. purely singular-continuous for $\lambda = 2$; and
3. pure-point with exponentially decaying eigenfunctions for $\lambda > 2$.

Then in 2005, twenty-one years after Kac's death, Avila and Jitomirskaya published the solution to the Ten Martini Problem [5]. In this paper we will focus on the 1999 results.

The almost Mathieu operator belongs to the class of quasiperiodic operators, which were first developed to explain planetary motion. The result of the Ten Martini Problem has direct implications in physics, as mentioned in [6]: the Lyapunov exponents, which measure the exponential growth rate of tangent vectors along orbits [7], on the spectrum of the almost Mathieu operator can be computed exactly. The purely absolutely continuous spectrum obtained for $\lambda < 2$ can be thought of as a representation of the delocalized electron system in electric conductors, or metals; on the other hand, the pure-point spectrum for $\lambda > 2$ represents an insulator system in which electron movement is limited. The physical significance of $\lambda = 2$ is yet unclear.

1.2 Basic Concepts from Analysis

Recall that metric spaces are special cases of topological spaces. Normed spaces are then special cases of metric spaces, and inner product spaces are special cases of normed spaces.

Definition 1.3 (Normed space, Banach space [8])**.** *A* normed space *X is a vector space with a norm defined on it. A* Banach space *is a complete normed space (complete in the the metric defined by the norm). Here a* norm *on a (real or complex) vector space X is a real-valued function on X whose value at an $x \in X$ is denoted by*

$$\|x\|$$

and which has the properties

1. $\|x\| \geq 0$
2. $\|x\| = 0 \Longrightarrow x = 0$
3. $\|\alpha x\| = |\alpha| \, \|x\|$
4. $\|x + y\| \leq \|x\| + \|y\|$

for $x, y \in X$ and $\alpha \in \mathbb{R}$. A norm on X defines a metric d on X which is given by

$$d(x, y) = \|x - y\| \tag{1.2}$$

and is called the metric induced by the norm*. The normed space just defined is denoted by $(X, \|\cdot\|)$ or simply by X.*

Definition 1.4 (Inner product space, Hilbert space [8]). *An* inner product space *is a vector space X with an inner product defined on X. The inner product induces a norm*

$$\|x\| = \sqrt{\langle x, x\rangle} \tag{1.3}$$

A Hilbert space *is an inner product space that is complete in the metric*

$$d(x, y) = \sqrt{\langle (x - y), (x - y)\rangle} \tag{1.4}$$

defined by the inner product. Here, an inner product *on X is a mapping of $X \times X$ into the scalar field K (e.g., $\mathbb{R}$ or $\mathbb{C}$) of X; that is, there is associated a scalar which is written*

$$\langle x, y\rangle$$

with every pair of vectors x and y. This scalar is called the inner product *of x and y, such that for all vectors $x, y, z \in X$ and scalar $\alpha \in \mathbb{R}$ we have*

1. $\langle x + y, z\rangle = \langle x, z\rangle + \langle y, z\rangle$
2. $\langle \alpha x, y\rangle = \alpha\langle x, y\rangle$
3. $\langle x, y\rangle = \overline{\langle y, x\rangle}$
4. $\langle x, x\rangle \geq 0$
5. $\langle x, x\rangle = 0 \Longrightarrow x = 0$

Note that these spaces may be either finite (e.g., $\mathbb{R}^n$, $\mathbb{C}^n$) or infinite (e.g., $l^2(\mathbb{Z})$, $l^2(\mathbb{N})$). Recall that

$$l^2(\mathbb{Z}) = \left\{ \text{infinite vectors} \begin{pmatrix} \vdots \\ u_{-1} \\ u_0 \\ u_1 \\ \vdots \end{pmatrix} \middle| \sum_{k=0}^{\infty} |u_k|^2 < \infty \right\}$$

where

$$u_k = \frac{\alpha + \beta i}{\sqrt{\alpha^2 + \beta^2}}$$

with $\alpha, \beta \in \mathbb{R}$. Now we define linear operators on spaces.

Definition 1.5 (Linear operator [8]). *In the case of vector spaces and, in particular, normed spaces, a mapping is called an* operator. *A* linear operator $T\colon X \to Y$ *is an operator such that for all $x, y \in X$ and $\alpha \in \mathbb{R}$,*

$$T(x + y) = Tx + Ty$$

and

$$T(\alpha x) = \alpha Tx$$

An operator may be expressed in whatever form is the most convenient for its domain space.

Example 1.6. *Consider an operator T acting on the space of infinite vectors*

$$T : l^2(\mathbb{Z}) \to l^2(\mathbb{Z})$$

Since the operator acts on infinite vectors, the infinite matrix form of T would be best suited for its domain.

A study of the spectrum of an operator can provide us with important information about the operator. The matrix representation of an operator is useful for studying its spectrum. In the case of finite operators, the matrix has a finite spectrum consisting solely of its eigenvalues; infinite operators such as the almost Mathieu operator have infinite spectra.

Definition 1.7 (Regular value, resolvent set, spectrum [8])**.** *Let $X \neq \{0\}$ be a complex normed space and $T\colon \mathfrak{D}(T) \to X$ a linear operator with domain $\mathfrak{D}(T) \subset X$. A* regular value *$\gamma$ of T is a complex number such that*

1. *$R_\gamma(T) = (\gamma I - T)^{-1}$ exists;*
2. *$R_\gamma(T)$ is bounded; and*
3. *$R_\gamma(T)$ is defined on a set which is dense in X.*

The resolvent set *$\rho(T)$ of T is the set of all regular values γ of T. Its complement $\sigma(T) = \mathbb{C} - \rho(T)$ in the complex plane is called the* spectrum *of T, containing* spectral values *$\gamma \in \sigma(T)$. Furthermore, the spectrum $\sigma(T)$ is partitioned into three disjoint sets:*

- *The* point spectrum *or* discrete spectrum *$\sigma_p(T)$ is the set such that $R_\gamma(T)$ does not exist. A $\gamma \in \sigma_p(T)$ is called an* eigenvalue *of T. In other words, a point spectrum contains only eigenvalues, which are discrete values.*
- *The* continuous spectrum *$\sigma_c(T)$ is the set such that $R_\gamma(T)$ exists and satisfies condition 3 but not 2. That is, $R_\gamma(T)$ is unbounded.*
- *The* residual spectrum *$\sigma_r(T)$ is the set such that $R_\gamma(T)$ exists (and may or may not be bounded) but does not satisfy condition 3; that is, the domain of $R_\gamma(T)$ is not dense in X.*

This project aims to gain a thorough, intuitive understanding of the almost Mathieu operator through a numerical study of its spectrum. Since it is difficult to intuitively understand infinite spectra, we use the software *Mathematica* to examine the spectra of finite truncations of the almost Mathieu operator.

Definition 1.8 (Truncated matrix)**.** *An $m \times m$* truncation *of an infinite matrix M is the $m \times m$ matrix composed of the first m rows and columns of M, and is denoted $H^{(m)}$.*

1.3 The Algorithm

The *Mathematica* algorithm used to define an $m \times m$ truncation $H^{(m)}$ of the almost Mathieu operator matrix is simple. It first builds an $m \times m$ matrix of 0's, then uses `For` loops to replace the appropriate elements, with `i` as the indexing term.

```
H = Table[0, {i, 1, m}, {j, 1, m}];
  For[i = 1, i < m, i++, H[[i, i + 1]] = 1; H[[i + 1, i]] = 1];
  For[i = 1, i <= m, i++,
    H[[i, i]] = N[2 lambda Cos[2 Pi (theta + i alpha)], 99]];
```

Because $\alpha \in \mathbb{I}$, the computer processor slows down when *Mathematica* attempts to store all the digits in its memory. To avoid unnecessarily taxing the machine, we use the command `N[..., 99]` to hold only the first 99 digits. Since this is primarily a numerical study, 99 digits are sufficient.

Numerical studies are limited to finite truncations of the operator matrix, so the spectrum is represented by the set of eigenvalues of the finite matrix. The *Mathematica* package includes the `Eigenvalues` command for calculating the eigenvalues of a matrix.

```
ev = Sort[N[Eigenvalues[H], 99]];
```

Note again the use of the `N[..., 99]` command to hold only a finite number of digits of each eigenvalue in the memory. We build the list `ev` to be the list of eigenvalues of `H`, sorted in increasing order. We sort the eigenvalues solely to facilitate later calculations. The eigenvalues can be plotted on the complex plane by separating the real and imaginary components into the two lists `real` and `imag`:

```
real = Table[Re[ev[[i]]], {i, 1, m}];
imag = Table[Im[ev[[i]]], {i, 1, m}];
```

In the case of the almost Mathieu Operator, all eigenvalues are real, so `imag` is a list of 0's. We plot the imaginary components of the eigenvalues against the real components using the `ListPlot` command:

```
ListPlot[Transpose[Join[{real}, {imag}]],
  PlotStyle -> {PointSize[.015], Hue[0.8]}]
```

Note that the eigenvalues of H are plotted on the real line. The primary focus of this paper will be to study the effect of λ on the length of the spectrum and on the distribution of eigenvalues.

Chapter 2

The Free Case

2.1 The Matrix

The general form of the almost Mathieu operator matrix is shown in (2.1), a symmetric tridiagonal matrix with $2\lambda\cos 2\pi(\theta + n\alpha)$ on the main diagonal, and 1's on either side of the main diagonal:

$$H_{\lambda,\alpha,\theta} = \begin{pmatrix} 2\lambda\cos 2\pi(\theta+\alpha) & 1 & 0 & \cdots \\ 1 & 2\lambda\cos 2\pi(\theta+2\alpha) & 1 & \cdots \\ 0 & 1 & 2\lambda\cos 2\pi(\theta+3\alpha) & \cdots \\ \vdots & \vdots & \vdots & \ddots \end{pmatrix} \tag{2.1}$$

It is clear from the results of [4] that λ is a crucial parameter to consider, since the value $\lambda = 2$ represents a transition point in the behavior of the spectrum. As we will consider λ almost exclusively in this project, we will notate the operator simply as H_λ. Now, we first examine the special case where $\lambda = 0$. Note that when $\lambda = 0$ we have

$$2\lambda\cos 2\pi(\theta + n\alpha) = 0 \tag{2.2}$$

so the main diagonal of the matrix becomes all 0's:

$$H_0 = \begin{pmatrix} 0 & 1 & 0 & 0 & 0 & \cdots \\ 1 & 0 & 1 & 0 & 0 & \cdots \\ 0 & 1 & 0 & 1 & 0 & \cdots \\ 0 & 0 & 1 & 0 & 1 & \cdots \\ 0 & 0 & 0 & 1 & 0 & \cdots \\ \vdots & \vdots & \vdots & \vdots & \vdots & \ddots \end{pmatrix} \tag{2.3}$$

Note that eigenvalue calculations for truncations of H_0 are relatively simple, so we call H_0 the *free case*.

Now, note that the irrationality of α is what makes H *almost* periodic. In the free case, however, this irrational value is cancelled by $\lambda = 0$, so H_0 is a periodic operator. In fact, H_0 is a *Mathieu operator*. Mathieu operators are the discrete version of the periodic Schrödinger operator.

2.2 Chebyshev Polynomials

Named after Pafnuty Chebyshev, Chebyshev polynomials are the solutions to the Chebyshev differential equations

$$(1-x^2)y'' - xy' + n^2 y = 0 \tag{2.4}$$
$$(1-x^2)y'' - 3xy' + n(n+2)y = 0 \tag{2.5}$$

The solutions of (2.4) are called *Chebyshev polynomials of the first kind*,denoted T_n. *Chebyshev polynomials of the second kind*, denoted U_n, are the solutions of (2.5). These polynomials are so ubiquitous that prominent mathematicians have been known to remark that "Chebyshev polynomials are everywhere dense in numerical analysis" [9]. We are particularly interested in the latter set of polynomials and their connection to the free Jacobi matrix.

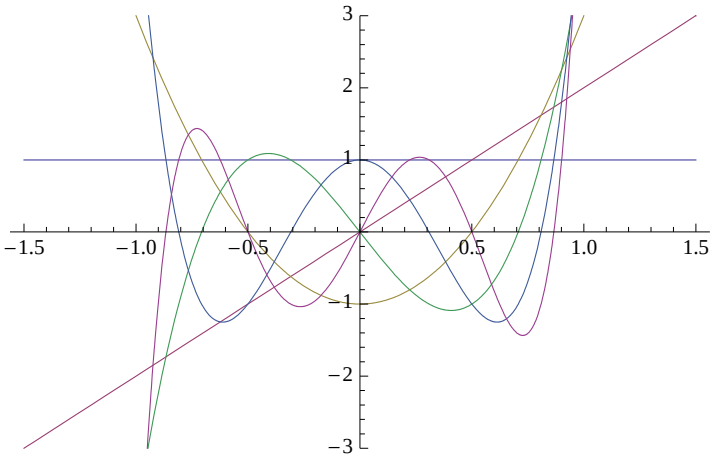

Figure 2.1: Chebyshev Polynomials of the Second Kind

Both kinds of Chebyshev polynomials can be recursively defined. U_n are defined by

$$U_0(x) = 1 \tag{2.6}$$
$$U_1(x) = 2x \tag{2.7}$$
$$U_{n+1}(x) = 2xU_n(x) - U_{n-1}(x) \tag{2.8}$$

to generate nth degree polynomials

$$U_0(x) = 1 \tag{2.9}$$
$$U_1(x) = 2x \tag{2.10}$$
$$U_2(x) = 4x^2 - 1 \tag{2.11}$$
$$U_3(x) = 8x^3 - 4x \tag{2.12}$$
$$U_4(x) = 16x^4 - 12x^2 + 1 \tag{2.13}$$
$$U_5(x) = 32x^5 - 32x^3 + 6x \tag{2.14}$$

and so on. The above functions are plotted in Figure 2.1.

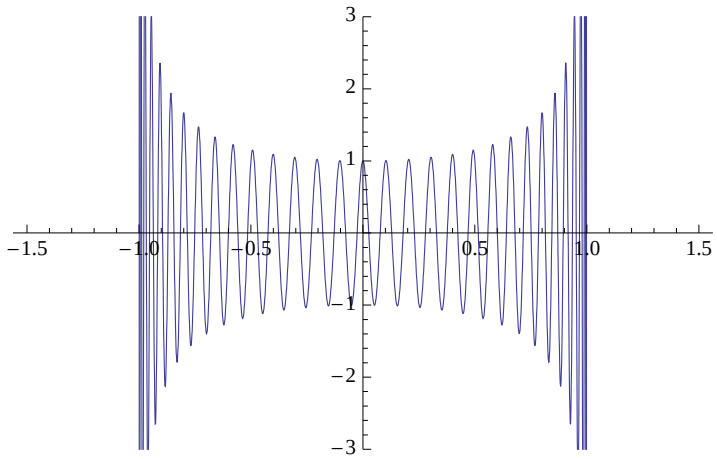

Figure 2.2: Zeros of $U_{60}(x)$

The reason for our fascination with Chebyshev polynomials is that $\{T_n\}$ and $\{U_n\}$ form sequences of orthogonal polynomials with respective weights

$$\omega_T(x) = \frac{1}{\sqrt{1-x^2}} \tag{2.15}$$

and

$$\omega_U(x) = \sqrt{1-x^2} \tag{2.16}$$

That is, for $\{U_n\}$ we have

$$\langle U_i, U_j \rangle = \frac{2}{\pi} \int_{-1}^{1} U_i(x) U_j(x) \sqrt{1-x^2} dx \tag{2.17}$$

$$= \begin{cases} 0 & \text{for } i \neq j \\ 1 & \text{for } i = j \end{cases} \tag{2.18}$$

Now, consider the orthogonal polynomials associated with the free case H_0. Since H_0 is a Jacobi matrix, we can use the recursion formula for defining orthogonal polynomials [10]

$$xP_n(x) = a_n P_{n+1}(x) + b_n P_n(x) + a_{n-1} P_{n-1}(x) \tag{2.19}$$

where $a_n \neq 0$, which can be arranged to

$$P_{n+1}(x) = \frac{x - b_n}{a_n} P_n(x) - \frac{a_{n-1}}{a_n} P_{n-1}(x) \tag{2.20}$$

with $P_0(x) = 1$ and $P_1(x) = x$. Here, $\{b_i\}$ are the elements in the main diagonal, and $\{a_i\}$ the elements of the second diagonals; so for H_0 we have $a_i = 1$ and $b_i = 0$, and

$$P_{n+1}(x) = xP_n(x) - P_{n-1}(x) \tag{2.21}$$

Note the similarities between (2.8) and (2.21). In fact, the two equations would be identical if $a_i = \frac{1}{2}$ and $b_i = 0$ for all i. That is, the orthogonal polynomials associated with the

operator

$$\frac{1}{2}H_0 = \begin{pmatrix} 0 & \frac{1}{2} & 0 & 0 & 0 & \cdots \\ \frac{1}{2} & 0 & \frac{1}{2} & 0 & 0 & \cdots \\ 0 & \frac{1}{2} & 0 & \frac{1}{2} & 0 & \cdots \\ 0 & 0 & \frac{1}{2} & 0 & \frac{1}{2} & \cdots \\ 0 & 0 & 0 & \frac{1}{2} & 0 & \cdots \\ \vdots & \vdots & \vdots & \vdots & \vdots & \ddots \end{pmatrix} \tag{2.22}$$

are exactly U_n, the Chebyshev polynomials of the second kind. Thus according to the relationship established in [10] between operator matrices and orthogonal polynomials, the zeros of Chebyshev polynomials of the second kind are the eigenvalues of $\frac{1}{2}H_0$, and it follows that these zeros are contained in $\sigma(\frac{1}{2}H_0) = \frac{1}{2}\sigma(H_0) = [-1, 1]$. For instance, see Figure 2.2. As n increases, the zeroes of U_n get more crowded together toward either end of the interval $[-1, 1]$.

Note now that the zeroes of orthogonal polynomials may be calculated to determine the exact spectrum of the almost Mathieu operator, rather than relying on the finitely truncated matrices to approximate them. An alternate recursion for the Chebyshev polynomials of the second kind is

$$U_n(x) = \frac{\sin\left[(n+1)\cos^{-1}x\right]}{(1-x^2)^{1/2}} \tag{2.23}$$

where $n = 1, 2, \ldots$. The zeroes of U_n are easily determined to be

$$x_n^{(k)} = \cos\frac{k}{\pi(n+1)} \tag{2.24}$$

for $k = 1, 2, \ldots, n$. Unfortunately, we did not realize this until quite late in the process, and thus were not able to take advantage of this useful discovery. Future continuations of this project should certainly include this, however, and start by finding the trigonometric form of the orthonormal polynomials for the almost Mathieu operator. Calculating the exact spectra would greatly improve the reliability of the numerical analysis.

2.3 The Spectrum of the Free Case

To begin our study of the free case, we write the *Mathematica* algorithm for the truncated matrix:

```
m = 40;
lambda = 7;
theta = Pi/7;
alpha = E/Pi;
H0 = Table[0, {i, 1, m}, {j, 1, m}];
  For[i = 1, i < m, i++, H0[[i, i + 1]] = 1; H0[[i + 1, i]] = 1];
  For[i = 1, i <= m, i++,
    H0[[i, i]] =
      N[2 (lambda /. lambda -> 0) Cos[2 Pi (theta + i alpha)], 99]];
```

Here, `H0` represents the $m \times m$ truncation of the free case, which we will denote $H_0^{(m)}$. Note that the command `/. lambda -> 0` overrides any previous values set for `lambda`, just for

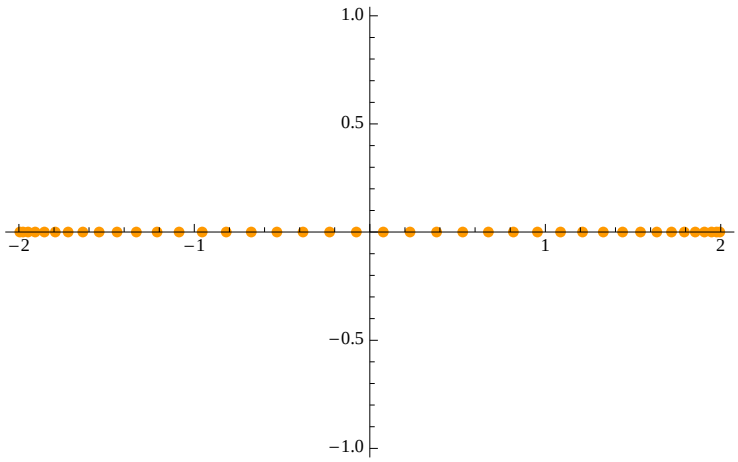

Figure 2.3: The eigenvalues of $H_0^{(40)}$

this instance, so that $\lambda = 0$ for this matrix definition. We will note here that we denote the list of real components of the eigenvalues of `H0` as `real0` in order to distinguish from `real` in future algorithms.

Note from Figure 2.3 that $\sigma(H_0^{(40)}) \subset [-2, 2]$. In fact, we can generalize this observation to say that $\sigma(H_0) = [-2, 2]$. To prove this we turn to [11] and first note that for each self-adjoint operator ϕ (up to unitary equivalence), we can define a multiplication operator M_ϕ with

$$\mathfrak{D}(M_\phi) = \{f \in \mathcal{H} | \phi f \in \mathcal{H}\} \tag{2.25}$$

such that for $f \in \mathfrak{D}(M_\phi)$

$$M_\phi f = \phi f \tag{2.26}$$

Recall that by the definition of spectrum, $\beta \in \sigma(M_\phi)$ if $(\beta I - M_\phi)$ is not invertible. Then $\beta \notin \sigma(M_\phi)$ if $(\beta I - M_\phi)^{-1}$ exists.

Now, when we apply $(\beta I - M_\phi)$ to $f(t)$ we have

$$[\beta I - M_\phi(t)](f(t)) = [\beta \cdot f(t)] - [\phi(t) \cdot f(t)] \tag{2.27}$$
$$= (\beta - \phi(t)) \cdot f(t) \tag{2.28}$$

This observation leads to the following lemma.

Lemma 2.1. *Let $\phi \neq 0$ be a self-adjoint operator with associated multiplication operator M_ϕ. Then $M_{1/\phi}$ is the inverse operator of M_ϕ.*

Proof. We will show that $M_\phi M_{1/\phi} = I = M_{1/\phi} M_\phi$. Note that

$$[M_\phi \cdot M_{1/\phi}](f) = M_{1/\phi}(\phi \cdot f) \tag{2.29}$$
$$= \frac{1}{\phi} \cdot \phi \cdot f \tag{2.30}$$
$$= f \tag{2.31}$$
$$= I(f) \tag{2.32}$$

Similarly, $M_{1/\phi} \cdot M_\phi(f) = I(f)$ so M_ϕ and $M_{1/\phi}$ are inverse operators. □

Note then that by Lemma 2.1, the inverse of the multiplication operator of $(\beta I - M_\phi)$ is

$$(\beta I - M_\phi)^{-1} = \frac{1}{\beta - \phi(t)} \tag{2.33}$$

which can only exist if $\beta \notin \mathfrak{R}(\phi)$. Thus $\beta \notin \mathfrak{R}(\phi)$ if and only if $\beta I - M_\phi$ is invertible, or $\beta \notin \sigma(M_\phi)$. Hence by the contrapositive,

$$\beta \in \sigma(\phi) \iff \beta \in \mathfrak{R}(\phi) \tag{2.34}$$

for self-adjoint operators ϕ, so

$$\sigma(\phi) = \mathfrak{R}(\phi) \tag{2.35}$$

This result proves significant later, when we show that H_0 is a multiplication operator.

We can study operators between spaces by taking the Fourier transforms of the spaces. In this case we have a Fourier function $\mathcal{F} : l^2(\mathbb{Z}) \to L^2(\mathbb{T})$ to give us this commutative diagram:

$$\begin{array}{ccc} l^2(\mathbb{Z}) & \xrightarrow{H} & l^2(\mathbb{Z}) \\ {\scriptstyle\mathcal{F}}\downarrow & & \downarrow{\scriptstyle\mathcal{F}} \\ L^2(\mathbb{T}) & \xrightarrow[T]{} & L^2(\mathbb{T}) \end{array}$$

Consider a vector

$$x = \begin{pmatrix} \vdots \\ u_{-2} \\ u_{-1} \\ u_0 \\ u_1 \\ u_2 \\ \vdots \end{pmatrix} \in l^2(\mathbb{Z}) \tag{2.36}$$

Applying H to x would yield

$$H(x) = \begin{pmatrix} \vdots \\ u_{-2} + u_0 \\ u_{-1} + u_1 \\ u_0 + u_2 \\ \vdots \end{pmatrix} \in l^2(\mathbb{Z}) \tag{2.37}$$

Now, recall that $\mathcal{F}$ transforms sequences to functions via

$$\mathcal{F}\begin{pmatrix} \vdots \\ u_{-1} \\ u_0 \\ u_1 \\ \vdots \end{pmatrix} = f_n(t) = \sum_{n\in\mathbb{Z}} u_n e^{int} \tag{2.38}$$

so for $x \in l^2(\mathbb{Z})$

$$[\mathcal{F}(x)](t) = \sum_{n\in\mathbb{Z}} u_n e^{int} \tag{2.39}$$

and

$$\begin{aligned}
[\mathcal{F}(H(x))](t) &= \sum_{n\in\mathbb{Z}} (u_{n-1} + u_{n+1}) e^{int} && (2.40)\\
&= \sum_{n\in\mathbb{Z}} u_n (e^{i(n-1)t} + e^{i(n+1)t}) && (2.41)\\
&= 2\cos t \sum_{n\in\mathbb{Z}} u_n e^{int} && (2.42)\\
&= 2\cos t \cdot [\mathcal{F}(x)](t) && (2.43)
\end{aligned}$$

Note that the result is the product of functions with

$$\begin{aligned}
&T : L^2(\mathbb{T}) \to L^2(\mathbb{T})\\
&T : f(t) \mapsto 2\cos t \cdot f(t)
\end{aligned}$$

so by (2.35), $\sigma(T) = \mathfrak{R}(T) = \mathfrak{R}(2\cos t) = [-2, 2]$. Furthermore, since $\mathcal{F}$ preserves operator spectrum, we have $\sigma(H) = \sigma(T) = [-2, 2]$, as supported by Figure 2.3.

Chapter 3

Standardizing Functions

It seems natural to consider the free matrix H_0 as a base case to which to compare the almost Mathieu operator H_λ with $\lambda \neq 0$. However, recall the distribution in Figure 2.3, of the eigenvalues of $H_0^{(40)}$, the 40×40 truncation of the free case. The distribution is not picket-fence – where all the distances between adjacent eigenvalues would be identical – which complicates comparisons, especially when there are only small discrepancies between plots. Furthermore, as λ increases, the length of $\sigma(H_n)$ also increases. Therefore we must first devise a standardizing function which, when applied, would map the eigenvalues of any truncated matrix to $[0, 1]$ while preserving the essential characteristics of the original distribution. This way, we will have a method for comparing the spectra of different matrices, especially in relation to that of the free case, which would ideally map to a picket-fence distribution. In this chapter, we will discuss such functions designed for the free case; subsequent chapters will explore the adaptations of these functions to the spectra of H_λ for other values of λ.

3.1 Redistribution of Points

In the first function we try, we treat the eigenvalues as a set of points to be redistributed. Since we want the eigenvalues of H_0 to be evenly distributed, we divide up the interval $[0, 1]$ into m subintervals of equal size, then assign the ith eigenvalue a_i (recall that $a_{i+1} > a_i$) to $\frac{i-1}{m}$ on $[0, 1]$:

$$f_0(a_i) = \frac{a_i}{a_i} \cdot \frac{i-1}{m} \tag{3.1}$$

The *Mathematica* code for this function builds a new list using f_0, which we call `f0`, applied to each of the eigenvalues.

```
f0 = Table[real0[[i]]/real0[[i]]*(i - 1)/m, {i, 1, m}];
```

The plot in Figure 3.1 of the the redistributed points shows that the function works as desired. To verify the visual observation, we can create a histogram showing how the distances between the points are distributed. Since we expect the distribution to be picket-fence, we should see a single bar over the interval containing the picket-fence distance.

First we build a list of the distances by subtracting $f_0(a_i)$ from $f_0(a_{i+1})$. We call this new list `drealfree`:

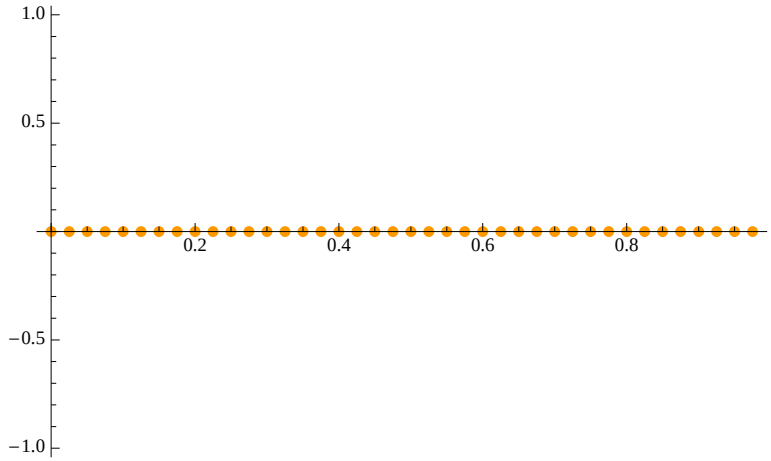

Figure 3.1: Standardizing function f_0 applied to $\sigma(H_0^{(40)})$

```
drealfree = Table[f0[[i + 1]] - f0[[i]], {i, 1, m - 1}];
```

Note that `drealfree` is a list of $m - 1$ values. Next, we assign a constant `picket` to be the length of each subinterval in a picket-fence distribution of eigenvalues, then defined a function `hist` to dictate the size of intervals to be used in the histogram.

```
picket = (Max[f0] - Min[f0])/m;
b = 20;
hist[first_, step_] := Table[first + (i - 1) step, {i, 2 b}];
```

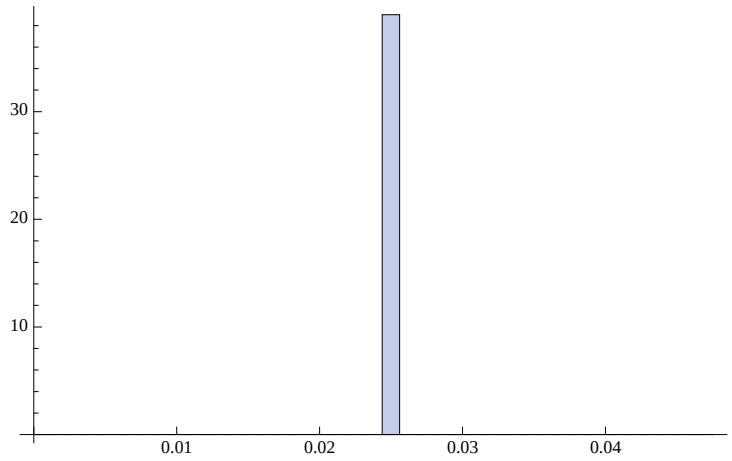

Figure 3.2: Distribution of the distances between $f_0(a_i)$ for $H_0^{(40)}$

Here, the variable `first` represents the smallest expected distance between points, which in our case will always be 0 since the initial sorting of eigenvalues guarantees distances greater than or equal to 0. The second variable `step` defines the size of the interval spanned by each histogram bar. The number `b` is used to determine the number of these intervals to be shown in the histogram. Finally, we will make the intervals smaller than the size expected for a

picket-fence distribution, to increase the accuracy of the information conveyed through the histogram. Finally, we plot the histogram of the distances between redistributed eigenvalues.

```
Histogram[drealfree, HistogramCategories -> hist[0, picket/b],
  HistogramRange -> {0, 500}]
```

Note that the histogram (Figure 3.2) shows a single bar as expected, indicating that the distances between the points are within $\frac{1}{b}$ of the picket-fence distances.

A more objective method of calculating the similarity of our distribution to the picket-fence distribution would be to calculate the variance within our set of distances. Recall from statistics [12] that the variance of a data set of size n is

$$s^2 = \frac{1}{n-1}\sum_{i=1}^{n}(x_i - \overline{x})^2 \tag{3.2}$$

where $\overline{x}$ represents the average value. In our case, x_i represents the distance between the ith and $i+1$th eigenvalues, and the mean distance would be the picket-fence distance $\frac{1}{m}$. Since there are $m-1$ of these distances, the variance calculation would look like

$$s^2 = \frac{1}{m-2}\sum_{i=1}^{m-1}(x_i - \overline{x})^2 \tag{3.3}$$

This calculation can be accomplished in *Mathematica* by the following code.

```
variance = 1/(m - 2) Sum[(drealfree[[i]] - picket)^2, i, 1, m - 1];
```

Thus small values of s^2 (i.e., close to 0) would indicate that the distances deviate very little from the picket-fence distance – in fact, for this method we obtain $s^2 = 0$, which tells us that the distribution is exactly picket-fence.

3.2 Cumulative Distribution Function

The other standardizing function that we consider is based on the theory of cumulative distribution functions, borrowed from statistics.

Definition 3.1. *The* cumulative distribution function (cdf) *of a distribution f is a monotone increasing function*

$$F_f : I \to [0,1] \tag{3.4}$$

such that

$$F_f(a) = \mathbb{P}(x \leq a) \tag{3.5}$$

for $a \in I$.

The probability is calculated as the area under the curve f on the interval I, up to the point a. The distribution f may be either continuous or discrete; the best-known distribution is the normal distribution, or the "bell curve." The cdf of the normal distribution is a sigmoidal curve.

Consider two normalized functions $f : I \to \mathbb{R}$ and $g : J \to \mathbb{R}$. That is,

$$\int_I f(x)dx = 1 \tag{3.6}$$

$$\int_J g(x)dx = 1 \tag{3.7}$$

Suppose $\varphi : I \to J$ is a map such that

$$F_f(a) = \int_{-\infty}^{a} f(x)dx = \int_{-\infty}^{\varphi(a)} g(x)dx = F_g(\varphi(a)) \tag{3.8}$$

Then

$$\varphi(a) = F_g^{-1}(F_f(a)) \tag{3.9}$$

This would be useful for our study if we could find a function $\varphi : \sigma(H) \to [0, 1]$ such that we could map the eigenvalues of any $H_\lambda^{(m)}$ to $[0, 1]$ while preserving the essential characteristic of their distribution so that we could compare the effects of different parameters.

Keeping this in mind, consider the distribution of $\sigma(H_0^{(40)})$ on $[-2, 2]$, in Figure 2.3. The eigenvalues get closer together toward either end of the spectrum, and farther apart in the middle. Since we would like to be able to use H_0 as a standard for comparison, a picket-fence distribution is desired for the free case on $[0, 1]$. Then $g(x)$ as defined above would be 1, so

$$F_g(x) = \int_{-\infty}^{0} 0dx + \int_0^x 1dx = x \tag{3.10}$$

and $F_g^{-1}(x) = x$. Thus we now have $\varphi_0 : [-2, 2] \to [0, 1]$ such that

$$\varphi_0(a) = F_g^{-1}(F_f(a)) \tag{3.11}$$

$$= F_f(a) \tag{3.12}$$

where F_f is the cdf of $\sigma(H_0)$. As we do not have an explicit mathematical function by which we plot the eigenvalues, we must describe the distribution of eigenvalues using the principle of a histogram. That is, we will divide $\sigma(H_0)$ into n subintervals, and count the number of eigenvalues in each subinterval. We accomplish this by first building a list `count` of n 0's. Then for each eigenvalue in the ith subinterval, we add 1 to the ith term in `count`.

```
count = Table[0, {i, 1, n}];
  For[r = 1, r <= m, r++,
    For[s = 1, s <= n, s++,
      If[(4 (s - 1))/n <= real0[[r]] + 2 < (4 s)/n,
        count[[s]] = count[[s]] + 1,
        count[[s]] = count[[s]]]]];
```

Note that we add 2 to the eigenvalues to shift the spectrum from $[-2, 2]$ to $[0, 4]$ in order to correctly index the subinterval containing x. To complete the definition of f we must normalize the area under the distribution "curve."

```
A = Sum[4/n count[[i]], {i, 1, n}];
norm = count/A;
```

Thus we build a new list `norm` of the normalized values of f. Next, before we can actually define the function $\varphi_0(x) = F_f(x)$, we must find a way to determine the subinterval containing x.

```
k[x_] := Ceiling[(n x)/4];
Phi[x_] := If[x <= Min[real],
  0,
  N[4/n Sum[norm[[i]], {i, 1, k[x]-1}]
    + norm[[k[x]]] (x - 4/n (k[x] - 1)), 99]];
```

We use `k[x]` to index the subinterval containing x. The `If` loop in `Phi` dictates that for values of x to the left of the minimum eigenvalue, we have $\varphi_0(x) = F_f(x) = 0$. This makes sense if we think of $F_f(x)$ as a measure of the area under the distribution curve up to x. If x is greater than the minimum rescaled eigenvalue, however, then we apply the calculation outlined in the "else" component of the `If` loop. That is,

$$\varphi_0(x) = \frac{4}{n}\left(\sum_{i=1}^{k-1} c_i\right) + (x - \frac{4}{n}(k-1))c_k \tag{3.13}$$

where k is the index of the subinterval containing x and c_i is the normalized count of eigenvalues in the ith subinterval. Now we can finally build a list `phi0` of φ_0 applied to the eigenvalues of H_0:

```
phi0 = Table[Phi[real[[i]]], {i, 1, m}];
```

and plot the new distribution. Note that the distribution in Figure 3.3 is not exactly picket-

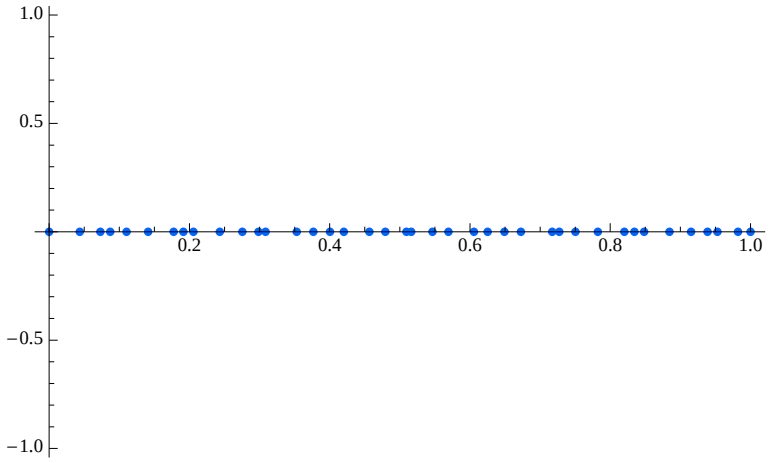

Figure 3.3: φ_0 applied to $\sigma(H_0^{(40)})$ with $n = 840$

fence, though close. The variance calculation given by

```
d = Table[phi0[[i + 1]] - phi0[[i]], {i, 1, m - 1}];
picket = (Max[phi0] - Min[phi0])/m;
variance = 1/(m - 2) Sum[(d[[i]] - picket)^2, i, 1, m - 1];
```

is 0.0001006, which tells us that the distribution is quite close to being picket-fence. The reason for the error is that the distribution function we are using depends on n, the number of subintervals. The greater the number of subintervals, the more we expect the distribution to resemble a curve. For instance, it is easy to spot the differences between the plots of eigenvalues generated with $n = 4$ and $n = 840$; also, note the similarity between Figures 2.3 and 3.4. Rather than plotting the distribution of distances between points, we can plot the

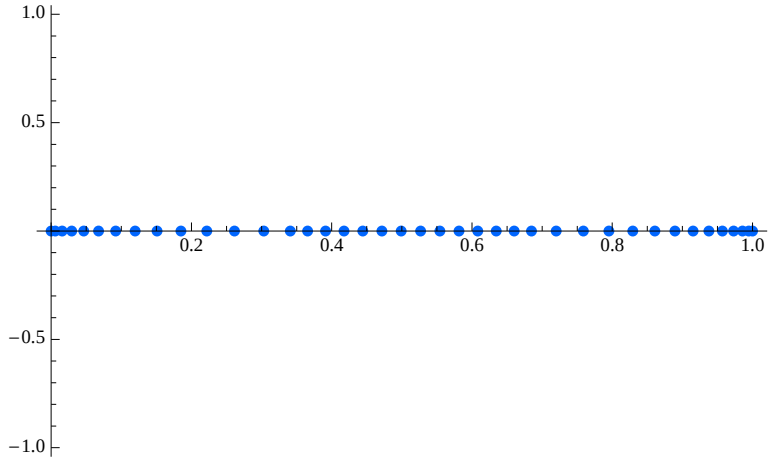

Figure 3.4: φ_0 applied to $\sigma(H_0^{(40)})$ with $n = 4$

actual distribution of the standardized eigenvalues in a histogram. We first define the size

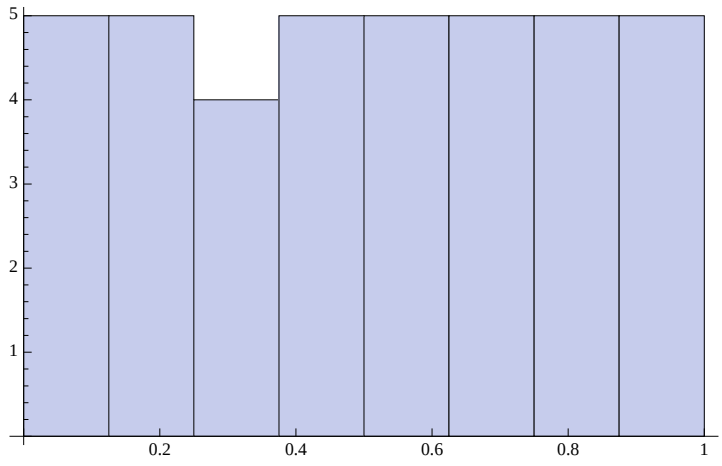

Figure 3.5: Distribution of $\varphi_0(\sigma(H_0^{(40)}))$ with $n = 840$

of the subintervals for the histogram

```
subint = 5/m;
```

then use the `hist` function again to plot the distribution of the points in `phi0`.

```
Histogram[phi, HistogramCategories -> hist[0, subint],
  HistogramRange -> {0, 500}]
```

Another statistical tool that we considered for describing and comparing the distributions of eigenvalues is the goodness-of- fit test. This method assumes a certain distribution – in our case, the picket-fence distribution – then compares how closely a given distribution fits the assumed distribution. This is accomplished by the formula

$$\chi^2 = \sum_{i=1}^{n} \frac{(\text{observed} - \text{expected})^2}{\text{expected}} \tag{3.14}$$

The weakness of this method is that rather than comparing each point in the spectrum to its corresponding point in the picket- fence distribution, we must divide the spectrum into n subintervals, then compare the number of eigenvalues in corresponding subintervals. Because the comparison values are then added up, the only information we can glean from a χ^2 value is how "close" a given distribution is to the picket-fence distribution – we lose crucial information about the actual distributions themselves. That is, if two distributions have different values of χ^2, then we know that they are different; however, two different distributions may have similar χ^2 values, and there is no way to distinguish between them from just their χ^2 values.

In chapter 4, we will generalize both of these standardizing functions to be applicable to non-free cases.

Chapter 4

Small Perturbations of the Free Case

4.1 Small Values of λ

Now that we have a better understanding of H_0, the free case, we examine the matrix generated with values of λ close to 0. Note that $\lambda \in [-\varepsilon, \varepsilon]$, does not make significant differences to the matrix – so we expect very small differences in the spectrum as well. Hence we consider the matrices generated with small λ to be small perturbations of the free case. To support these intuitions, we standardize the spectra of the new matrices using adaptations of the methods outlined in Chapter 3, and compare them to that of the free case. Note that as $\lambda \sim 0$ does not significantly affect the length of $\sigma(H_\lambda)$, few changes are required to adapt the standardizing functions.

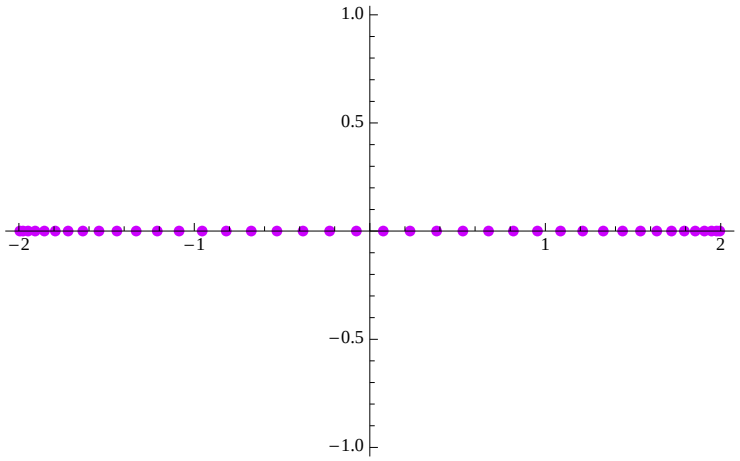

Figure 4.1: Eigenvalues of $H_{0.001}^{(40)}$

4.2 Redistribution of Points

Recall that for the standardizing function f_0, we assigned the ith eigenvalue to $\frac{i-1}{m}$ by (3.1). The *Mathematica* algorithm constructed a list `f0` of these re-assigned eigenvalues. We adapt

this to make the generalized function f:

$$f(b_i) = \frac{b_i}{a_i} \cdot \frac{i-1}{m} \tag{4.1}$$

where $b_i \in \sigma(H_{\lambda \neq 0})$ and $a_i \in \sigma(H_0)$. The new algorithm makes a list `f`:

```
f = Table[real[[i]]/real0[[i]]*(i - 1)/m, {i, 1, m}];
```

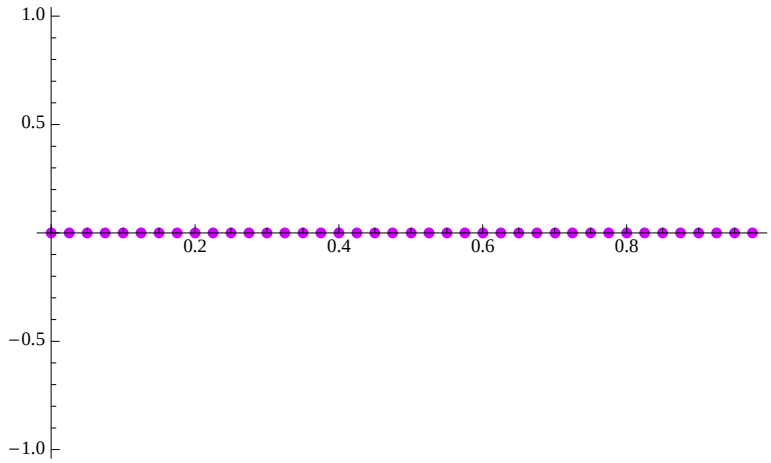

Figure 4.2: Standardizing function $f_0(a_i)$ applied to $H^{(40)}_{0.001}$

Note that this function is dependent on the spectrum of H_0, which makes sense intuitively because we want to use $\sigma(H_0)$ as a standard of comparison. However, as we see in the next chapter, this reasoning fails for larger λ because the length of $\sigma(H_\lambda)$ exceeds that of $\sigma(H_0)$.

The algorithm outlined above yields the same histogram as that in Figure 3.2 for $\lambda \leq 0.0009$. For larger values than 0.0009, we begin to notice some changes, and the utility of histograms becomes apparent. The histogram in Figure 4.3 indicates a change in the

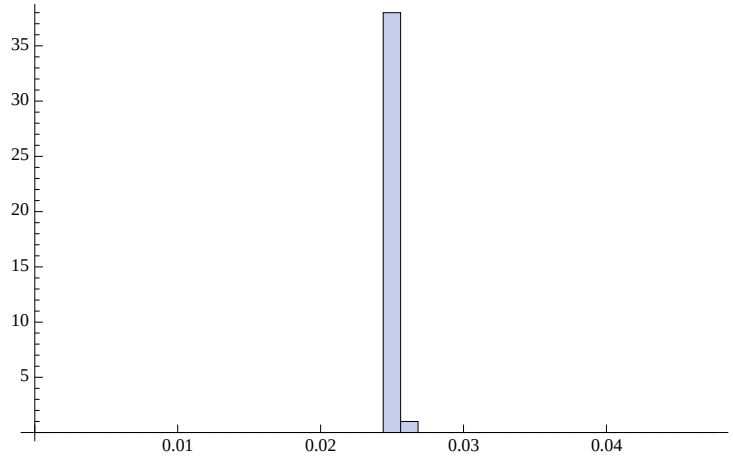

Figure 4.3: Distribution of the distances between $f_0(a_i)$ for $H^{(40)}_{0.001}$

spectrum, but it is difficult to detect such small changes by eye. The variance for $\lambda = 0.001$

is quite small ($s^2 = 4.159 \times 10^{-7}$) but the histogram can begin to detect the changes in the distribution on this level.

Figures 4.1 and 4.2 show the eigenvalues of $H_{0.001}^{(40)}$ before and after the standardizing function $f_0(a_i)$ is applied to them, respectively. The differences between these and the respective plots for $H_0^{(40)}$ – Figures 2.3 and 3.1 – are almost imperceptible to the eye. As λ increases, the standardized distribution of eigenvalues becomes less of a picket-fence distribution.

4.3 Cumulative Distribution Function

Because the values of λ considered for this chapter do not significantly affect the length of the spectrum, we can use the cdf `Phi` as defined in the previous chapter. The only difference is that the matrix `H0` and the list `real0` are replaced by `H` and `real`, respectively.

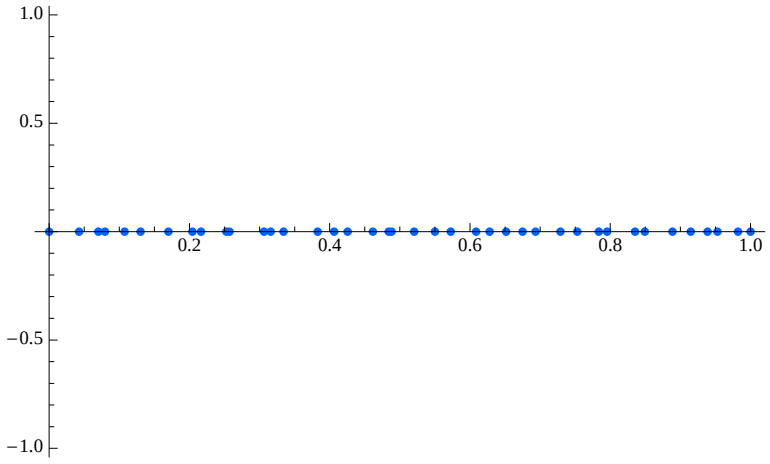

Figure 4.4: φ applied to $\sigma(H_{0.015}^{(40)})$ with $n = 840$

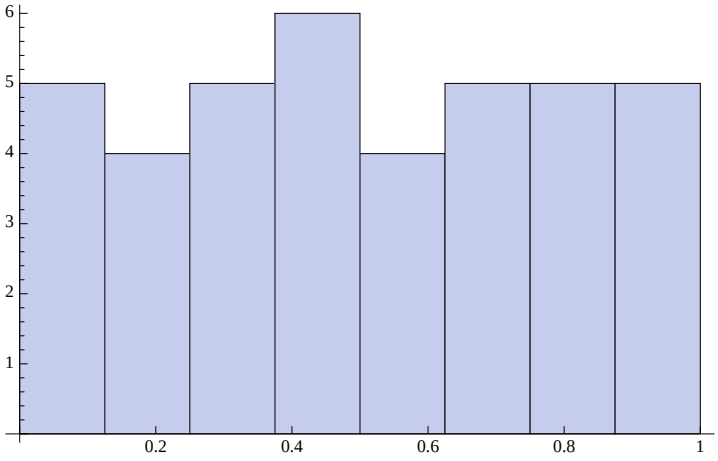

Figure 4.5: Distribution of $\varphi(\sigma(H_{0.015}^{(40)}))$ with $n = 840$

The function φ seems to be less sensitive to the differences in the spectrum wrought by small changes in λ. The the standardized distribution shows very little apparent change until λ reaches 0.015, and even then, it is only with the aid of the histogram that we are able to notice this difference at all. We have $s^2 = 0.0001309$ for $\lambda = 0.015$, which is significantly greater than the variance required before a change is detectible by histogram in the redistribution method. However, the cdf method is far more generalizable than the other, as we see in the next chapter.

Chapter 5

Larger Perturbations of the Free Case

5.1 Large Values of λ

The larger values of λ present a problem for the standardizing codes presented in Chapter 3 because the spectrum increases. That is,

$$\sigma(H_\lambda) > [-2, 2] \tag{5.1}$$

for large λ. This is because λ influences the diagonal elements of H_λ. Thinking about this heuristically, we notice that when $\lambda = 0$, the diagonal contains only 0's, so only the second diagonals of 1's figure in the calculation for eigenvalues. However, as λ increases, the main diagonal eventually dominates. From (1.1) we see that since $\cos 2\pi(\theta + n\alpha) \in [-1, 1]$, only the size of 2λ will have a significant impact on the values in the diagonal. For $\lambda \sim 1$, it is unclear which diagonals would be dominant; thus it makes sense that $\lambda = 2$ would mark the transition from a purely a.c. spectrum to a pure-point one, as proven in [4].

Using *Mathematica* we show in Figure 5.1 that $\sigma(H_1)$ is approximately

$$[-(2\lambda + 1), (2\lambda + 1)] \tag{5.2}$$

and that as λ increases, the second diagonals' influence on the size of the spectrum decreases. This observation relates to a theorem in [6]:

Theorem 5.1 (Aubry-Andre conjecture)**.** *The measure of the spectrum of $H_{\lambda,\alpha,\theta}$ is equal to $|4 - 2|\lambda||$ for all irrational α and all λ.*

Now, there is some discrepancy between this theorem and Theorem 5.1, since the theorem dictates that the spectrum have measure 0 for $\lambda = 2$, but the plot in Figure 5.1 clearly disagrees with this result. In fact, the plots do not obey the theorem for λ in approximately the $[1, 4]$ range. This discrepancy may simply be an effect of the transition from dominance by the second diagonals to the main-diagonal dominance, as discussed previously. Alternately, the problem may lie with the limits of computer software and processor capacity – that is, it is likely that somewhere between the numerical calculations and approximations, the irrationality of α was lost, rendering results that are inconsistent with theory.

5.2 Redistribution of Points

Recall that $\sigma(H_\lambda) > [-2, 2]$. Hence for certain i,

$$\frac{b_i}{a_i} \notin [0, 1] \tag{5.3}$$

and thus

$$\frac{b_i}{a_i} \cdot \frac{i-1}{m} \notin [0,1] \tag{5.4}$$

We were unable to discover a viable solution to overcome this problem and adapt f_0 to the general case. Therefore we approached the standardization from a different angle and conceived of the cdf method.

5.3 Cumulative Distribution Function

We considered two possible ways to adapt φ_0 to general cases. In the first method we defined a value d such that

$$d = \max_i \{a_i\} - \min_i \{a_i\} \tag{5.5}$$

$$= a_m - a_1 \tag{5.6}$$

and used it to define the length of the spectrum. Thus all instances of "4" in the original algorithm were replaced with d. This solution created an unforeseen problem, namely that because of the numerical approximations involved in the algorithm, the *Mathematica* calculations generated very small numbers such as 10^{-99} instead of 0's, which resulted in failure to compute.

Rather than wrestle with these errors, we chose to simply add an extra component to the algorithm for φ_0, scaling the eigenvalues of H_λ to $[0,4]$ then applying exactly the same calculations as for the free case. After the `real` list is constructed, we define a new list `rescale` of the scaled eigenvalues.

```
rescale = Table[0, {i, 1, m}];
  rescale[[1]] = 0;
  For[i = 2, i <= m, i++,
    rescale[[i]] = 4 (real[[i]] - real[[1]])/(real[[m]] - real[[1]])];
```

The subsequent calculations draw values from `rescale` rather than from `real`.

```
count = Table[0, {i, 1, n}];
  For[r = 1, r <= m, r++,
    For[s = 1, s <= n, s++,
      If[(4 (s - 1))/n <= rescale[[r]] < (4 s)/n,
        count[[s]] = count[[s]] + 1,
        count[[s]] = count[[s]]]]];
```

Notice here that there is no need to add 2 to the scaled eigenvalues, since the spectrum is already contained in $[0,4]$ rather than in $[-2,2]$. The rest of the algorithm is unchanged from the original.

It is possible to combine the commands outlined above into a single function given any set of parameters, using the *Mathematica* command `Module`. This way, one may simply input the values of m and n and generate either a plot of the standardized eigenvalues or a histogram of their distribution. Please refer to Appendix A for the full algorithms for `standardizef` and `standardizecdf`.

Now, recall the results published by Jitomirskaya, mentioned at the very beginning of this paper. According to those results, we should see a fairly even distribution of points for $\lambda < 2$ and discrete clusters of points for $\lambda > 2$. However, Figure 5.1 belies these expectations, as the clumping of points is much more obvious for $\lambda = 1$ than for $\lambda = 4$, for instance. There are several explanations for this discrepancy between the theoretical and numerical results. One that had been previously mentioned is that because of the current limitations of processors, we have had to resort to numerical approximations of irrational numbers. This is probably the biggest contributor of errors, since the theoretical conclusions are based on the assumption that α is irrational.

Another possibility is that the finitely truncated matrices have different properties than the infinite matrix operator. Since the eigenvalues of our finite matrices are only poor approximations of the full spectra of the infinite matrices, it is certainly plausible that they would embody very different properties. This last problem may be overcome using the zeroes of orthogonal polynomials to calculate the exact spectra.

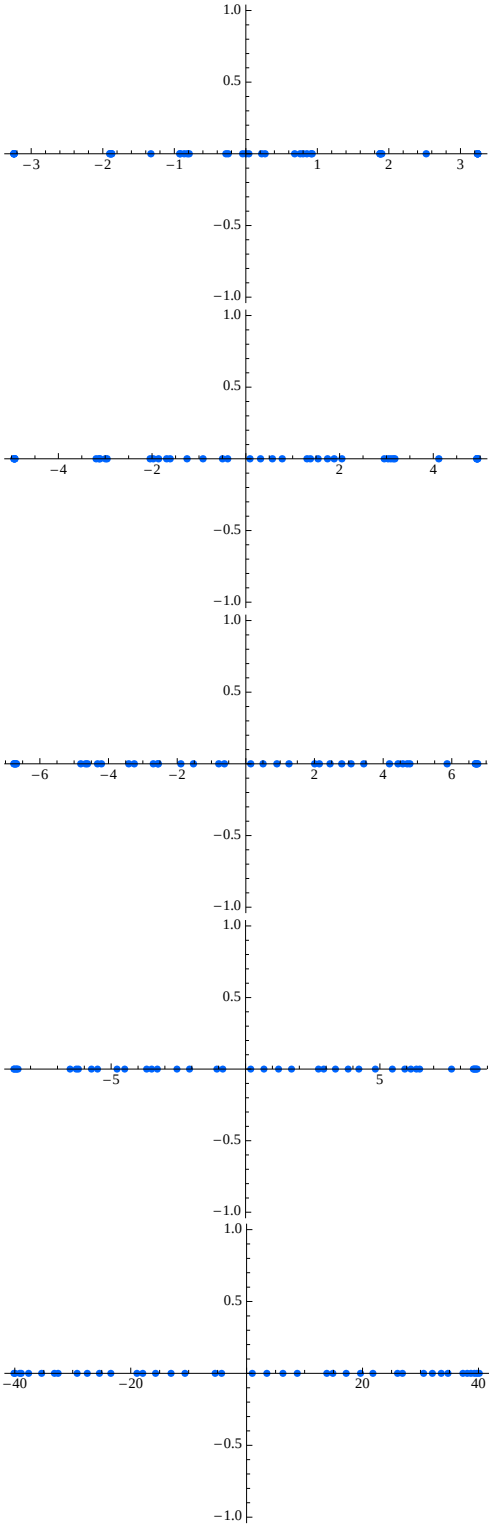

Figure 5.1: The spectra of $H_\lambda^{(40)}$ for $\lambda = 1, 2, 3, 4,$ and 20

Appendix A

Combined Algorithms

The `Module` command allows us to define local variables then combine all the steps into a single function. The inputs for both of the following functions are m and n. `Modlue` requires two parts, separated by a comma. The first is the list of variables to be locally defined in the function. The second part is all the definitions and operations that are part of the function, and these must be separated by semicolons. The "output" of the function is the last item in the second part of the module.

A.1 Redistribution of Points

The `standardizef` function will have three outputs: a plot and the calculated variance of the redistributed eigenvalues, and a histogram of the distances between eigenvalues.

```
standardizef[m_, n_] :=
  Module[
    {H0, H, ev0, real0, ev, real, imag, f, plot, hist, d, picket,
      variance, b, distances},

    H0 = Table[0, {i, 1, m}, {j, 1, m}];
      For[i = 1, i < m, i++, H0[[i, i + 1]] = 1; H0[[i + 1, i]] = 1];
      For[i = 1, i <= m, i++,
      H0[[i, i]] = N[2 (lambda /. lambda -> 0)
          Cos[2 Pi (theta + i alpha)], 99]];

    H = Table[0, {i, 1, m}, {j, 1, m}];
      For[i = 1, i < m, i++, H[[i, i + 1]] = 1; H[[i + 1, i]] = 1];
      For[i = 1, i <= m, i++,
        H[[i, i]] = N[2 lambda Cos[2 Pi (theta + i alpha)], 99]];

    ev0 = Sort[N[Eigenvalues[H0], 99]];
    real0 = Table[Re[ev0[[i]]], {i, 1, m}];

    ev = Sort[N[Eigenvalues[H], 99]];
    real = Table[Re[ev[[i]]], {i, 1, m}];
    imag = Table[Im[ev[[i]]], {i, 1, m}];
```

```
    f = Table[real[[i]]/real0[[i]] * (i - 1)/m, {i, 1, m}];

    plot = ListPlot[Transpose[Join[{f}, {imag}]],
      PlotStyle -> {PointSize[.012], Hue[0.8]}];

    d = Table[f[[i + 1]] - f[[i]], {i, 1, m - 1}];
    picket = (Max[f] - Min[f])/m;
    variance = 1/(m - 2) Sum[(d[[i]] - picket)^2, {i, 1, m - 1}];

    b = 20;
    hist[first_, step_] := Table[first + (i - 1)*step, {i, 2 b}];
    distances = Histogram[d, HistogramCategories -> hist[0, picket/b],
      HistogramRange -> {0, 1000}];

    Print[plot];
    Print[variance];
    Print[distances]]
```

A.2 Cumulative Distribution Function

The `standardizecdf` function uses the cdf method to standardize the eigenvalues. It outputs a plot, a histogram of the distribution, and the calculated variance of the standardized eigenvalues, as well as the histogram of distances.

```
standardizecdf[m_, n_] :=
  Module[
    {H, ev, real, imag, rescale, count, A, normalized, k, Phi, phi, plot,
      subint, hist1, distribution, d, picket, variance, b, hist2, distances},

    H = Table[0, {i, 1, m}, {j, 1, m}];
      For[i = 1, i < m, i++, H[[i, i + 1]] = 1; H[[i + 1, i]] = 1];
      For[i = 1, i <= m, i++,
        H[[i, i]] = N[2 lambda Cos[2 Pi (theta + i alpha)], 99]];

    ev = Sort[N[Eigenvalues[H], 99]];
    real = Table[Re[ev[[i]]], {i, 1, m}];
    imag = Table[Im[ev[[i]]], {i, 1, m}];

    rescale = Table[0, {i, 1, m}];
      rescale[[1]] = 0;
      For[i = 2, i <= m, i++,
        rescale[[i]] = 4 (real[[i]] - real[[1]])/(real[[m]] - real[[1]])];

    count = Table[0, {i, 1, n}];
      For[r = 1, r <= m, r++,
        For[s = 1, s <= n, s++,
          If[(4 (s - 1))/n <= rescale[[r]] < (4 s)/n,
            count[[s]] = count[[s]] + 1,
```

```
        count[[s]] = count[[s]]]]];

A = Sum[4/n count[[i]], {i, 1, n}];
norm = count/A;

k[x_] := Ceiling[(n x)/4];

Phi[x_] := If[x <= Min[real],
  0,
  N[4/n Sum[norm[[i]], {i, 1, k[x]-1}]
    + norm[[k[x]]] (x - 4/n (k[x] - 1)), 99]];

phi = Table[Phi[real[[i]]], {i, 1, m}];

plot = ListPlot[Transpose[Join[{phi}, {imag}]],
  PlotStyle -> {PointSize[.012], Hue[0.6]}];

subint = 5/m;

hist1[first_, step_] := Table[first + (i - 1)*step, {i, m/5 + 1}];

distribution = Histogram[phi, HistogramCategories -> hist1[0, subint],
  HistogramRange -> {0, 500}];

d = Table[phi[[i + 1]] - phi[[i]] , {i, 1, m - 1}];
picket = (Max[phi] - Min[phi])/m;
variance = 1/(m - 2) Sum[(d[[i]] - picket)^2, {i, 1, m - 1}];

b = 20;
hist2[first_, step_] := Table[first + (i - 1)*step, {i, 2 b}];
distances = Histogram[d, HistogramCategories -> hist2[0, picket/b],
  HistogramRange -> {0, 1000}];

Print[plot];
Print[distribution];
Print[variance];
Print[distances]]
```

Bibliography

[1] Folland, Gerald B. *Real analysis. Modern techniques and their applications*. Second edition. New York: Pure and Applied Mathematics – Wiley-Interscience Publication, 1999.

[2] Barile, Margherita and Weisstein, Eric W. "Cantor Set." From MathWorld – A Wolfram Web Resource. http://mathworld.wolfram.com/CantorSet.html.

[3] J. Puig, *Cantor Spectrum for the Almost Mathieu Operator. Corollaries of localization, reducibility, and duality*, eprint arXiv:math-ph/0309004v1 (2003).

[4] S. Jitomirskaya, *Metal-insulator transition for the almost Mathieu operator*, Ann. of Math. (2) 150 (1999), no. 3, 1159-1175.

[5] Avila, A. and S. Jitomirskaya, *The Ten Martini Problem*, eprint arXiv:math/0503363 (2005).

[6] S. Jitomirskaya, *Ergodic Schrödinger Operators (on one foot)*, Proceedings of Symposia in Pure Mathematics 76.2 (2007), 613-647.

[7] Brin, M. and G. Stuck. *Introduction to Dynamical Systems*. Cambridge, UK: Cambridge University Press, 2002.

[8] Kreyszig, E. *Introductory Functional Analysis with Applications*. New York: John Wiley & Sons, Inc., 1978.

[9] Mason, J.C. and D.C. Handscomb. *Chebyshev Polynomials*. Boca Raton, FL: Chapman & Hall/CRC, 2002.

[10] Simon, B. *The classical moment problem as a self-adjoint finite difference operator*, Adv. Math. 137 (1998), no. 1, 82-203.

[11] Carmona, R. and J. Lacroix, *Spectral Theory of Random Schrödinger Operators*. Boston: Birkhäuser, 1990.

[12] Moore, D.S. and G.P. McCabe, *Introduction to the Practice of Statistics*. Third edition. New York: W.H. Freeman and Company, 1999.